Magnetic Resonance Imaging of Anatomical Tissue and Vascular Layers in the Cat Retina

Q. Shen[1], H. Cheng[1], T. Chang[2], G. Nair[1], R. Shonat[3], T. Q. Duong[1]

[1]Yerkes Imaging Center, Emory University, Atlanta, GA, United States, [2]University of Massachusetts Medical School, Worcester, MA, United States, [3]Biomedical Engineering, Worcester Polytechnic Institute, Worcester, MA, United States

Introduction The neural retina is about 200-300 μm thick, is highly structured, and can be approximated into three major cell layers: an outer photoreceptor layer, a middle bipolar cell layer, and an inner ganglion cell layer. Bipolar cells are the primary synaptic link between the photoreceptors and the ganglion cells. Within the bipolar cell layer, there are also horizontal and amacrine cells that span horizontally. Histological studies suggest that the cell density is highly localized to the middle layer of the retina. The retina is nourished by two separate blood supplies: the retinal and choroidal vasculatures. The retinal vasculature exists primarily within the inner ganglion cell layer, but does project a deep planar capillary bed into the bipolar cell layer. The choroidal vasculature does not exist within any retinal layer, but rather is located directly beneath the photoreceptor layer, sandwiched between the sclera and pigment epithelial cell layer. There are also marked differences between the retinal and choroidal vasculature. Choroidal blood flow is many times higher than the retinal blood flow and is much less responsive to many blood flow regulating factors. In addition, many vascular diseases of the eye, including diabetic retinopathy, glaucoma and macular degeneration, are thought to preferentially affect only one vasculature. The ability to separately resolve these retinal tissue layers, including the two distinct vasculatures, non-invasively could have many important applications.

The goal of this study was to explore the optimization of T_2, diffusion, and contrast-enhanced T_1 imaging to resolve anatomical and vascular layers in the retina by sensitizing different MRI contrast to the heterogeneous local biophysical and biochemical environment in different retinal layers. Furthermore, since the *retinal* and *choroidal* vasculatures largely define the boundaries of the retina, Gd-DTPA contrast-enhanced T_1-weighted MRI was also used to visualize these vessel layers.

Methods Multiple survival experiments were performed on 5 female adolescent cats (0.7–1.4kg). The animal was mechanically ventilated under isoflurane (1.25-1.5%) during MRI. End-tidal CO_2 was continuously monitored. Contact lens or ophthalmic gel was used to prevent dryness of the cornea. The animal was placed in a cradle and restrained in a normal postural position. Rectal temperature was maintained at 38±0.5°C. Fluid supplement were administered. In some experiments, contrast-enhanced imaging was also performed in which Gd-DTPA was administered intravenously (0.4mL/kg from a standard 0.5M bottle) via the catheterized forepaw vein.

T_2-, T_1- and diffusion-weighted images (DWI) were acquired on a 4.7T Bruker scanner with matrix =256×256, FOV = 2.56×2.56cm (100x100μm), and a slice thickness=1.5mm. T_2-weighted images were acquired with the RARE pulse sequence, $TE_{effective}$= 40, 52, 72, 100ms and TR = 4s. DWI was acquired with diffusion-sensitive gradients applied along the x, y or z direction separately, TR = 2.5s, TE = 43ms, Δ = 20 ms, δ = 3.5ms, b = 6,504s/mm^2. T_1-weighted images were acquired using RARE with a short TR=1500 ms, and $TE_{effective}$= 40 ms). In some studies, 50x100μm in-plane resolutions were also acquired by reducing half of the readout FOV.

Results & Discussions Fig. 1 shows the T_2-weighted images at 100x100μm resolution for three different radial orientations with respect to the center of the eye. The image at 0^o is the sagittal slice and images at 10^o and 20^o extend towards the optic nerve, which lies nasally to the sagittal slice. Multiple "layers" were observed in the retina (~4-5 pixels, 100x100μm), as indicated by the alternating bright, dark and bright strips on the T_2-weighted images. The short T_2 in the middle strip is consistent with the relatively higher cell density in the middle layer of the retina. These layered structures disappeared in and around the optic nerve head. The retina at the optic nerve head appeared slightly protruded above the surrounding retinal surface. Higher spatial resolution (50x100μm) T_2- and diffusion-weighted images are shown in **Fig. 2**. The layer contrast on DWI_x was markedly different from those of DWI_y and DWI_z, indicative of diffusion anisotropy. Across the thickness of the retina (vertical direction), there were approximately nine 50-μm pixels. The group-average, T_2, $ADC_{//}$ and $ADC_{\perp}$ along the different strips of the retina and the vitreous humor are summarized in **Table 1**. Note that bright DWI should yield low ADC but high ADC was observed. This is because the DWI signals were dominated by water spin density. The middle strip showed the smallest and the vitreous showed the largest T_2 and ADC as expected. $ADC_{//}$ and $ADC_{\perp}$ were not statistically different for the vitreous humor and inner strip ($P>0.05$) but were statistically different for the middle and outer strips ($P<0.05$). Surprisingly, $ADC_{//}$ of the outer strip was markedly higher than other strips and was similar to the ADC of the vitreous, likely due to blood flow contribution of the choroidal vessels that runs tangential to the outer retinal surface. $ADC_{//}$ of the middle strip was high compared to $ADC_{\perp}$ of the middle strip, likely due to the partial-volume effect of the high $ADC_{//}$ of the outer strip. The retinal thickness, including the retinal/choroid complex, was estimated to be 400-500 μm, consistent with those reported previously using invasive techniques.

To further corroborate the classification of different retinal tissue strips by MRI, contrast-enhanced imaging was performed using Gd-DTPA. Pre-contrast spin-echo T_1-weighted images (with some T_2 weighting) also showed three distinct strips. T_1-weighted images of the retina after Gd-DTPA administration showed marked enhancement of the anterior segment of the eye due to the high permeability of the ciliary body (**Fig. 3**). Extra-ocular enhancement was also observed. Subtraction of post- and pre-contrast T_1-weighted images showed significant signal enhancement on either side of the retina, with the outer strip being markedly more enhanced and appeared thicker (1-2 pixels) than the inner strip (1 pixel). The middle strip of the retina and the vitreous were not significantly enhanced.

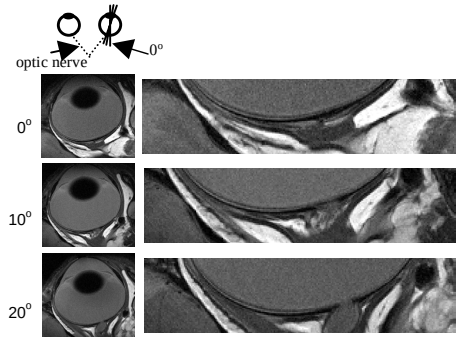

Fig 1. Scout imaging

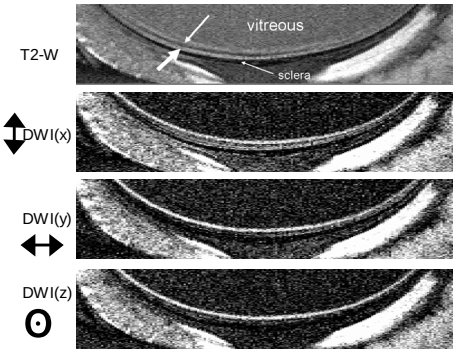

Fig 2. 50×100μm T_2-weighted and DWI images

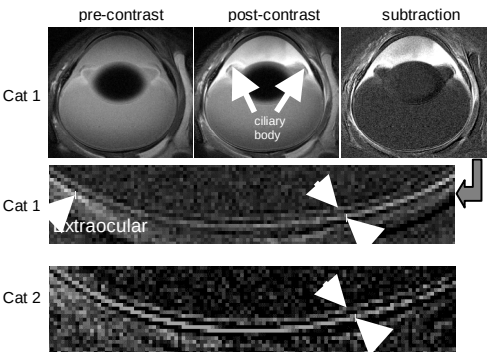

Fig 3. Contrast-enhanced imaging

Table 1 Group-average T_2, $ADC_{//}$ & $ADC_{\perp}$.

N=5		T_2 (ms)	$ADC_{//}$ ($x10^{-3}mm^2/s$)	$ADC_{\perp}$ ($x10^{-3}mm^2/s$)
Vitreous humor		218 ± 12	2.73 ± 0.22	2.66 ± 0.22
Retina	"inner"	98 ± 9	1.1 ± 0.2	0.74 ± 0.1
	"middle"	48 ± 5	1.2 ± 0.3 *	0.67 ± 0.1 *
	"outer"	95 ± 6	3.3 ± 0.7 *	1.2 ± 0.2 *

Conclusions This study demonstrates the visual resolution of three distinct strips in the cat retina using T_2-weighted, diffusion-weighted, and Gd-DTPA contrast-enhanced MRI, although there was some partial-volume effect. Non-invasive MRI of the retina offers rich and complementary anatomical tissue and vascular information because of its flexible and excellent soft tissue contrasts and its three-dimensional imaging capability. The potential for layer-specific imaging of the retina to yield physiological (such as separate blood flow and oxygenation changes in the retinal and choroidal vasculatures) and functional information in the same setting could substantially enhance the diagnostic utility of high-resolution MRI in the retina.